Malaya Journal of Matematik, Vol. 6, No. 2, 428-434, 2018

https://doi.org/10.26637/MJM0602/0021

Effect of space and temperature dependent internal heat generation/absorption on Casson fluid flow in the presence of an inclined magnetic field

P. Renuka[1], B. Ganga [2] and A.K. Abdul Hakeem[3]*

Abstract

The present study focuses on the inclined magnetic field effect on Casson fluid flow over a stretching sheet with non-uniform heat source/sink. The velocity slip boundary conditions are considered. A similarity transformation of governing equation is used to reduce into a non-dimensional form. The flow and thermal equations are derived and solved analytically by using confluent hypergeometric function and numerically by using shooting iteration technique together with Runge-Kutta fourth order. Results for various flow characteristics are presented through graphs. It is found that increasing the values of the inclined magnetic field enhances the thermal boundary layer. Also observed that the increasing value of non-uniform heat source/sink parameter increase the thermal boundary layer thickness.

Keywords

Casson fluid, Inclined magnetic field, Non-uniform heat source/sink, Slip flow, Thermal radiation.

AMS Subject Classification

76D05, 76W05, 80A20.

[1] *Department of Mathematics, Erode Sengunthar Engineering college, Erode - 638 057, India.*

[2] *Department of Mathematics, Providence College for Women, Coonoor - 643 104, India.*

[3] *Department of Mathematics, Sri Ramakrishna Mission Vidyalaya College of Arts and Science, Coimbatore - 641 020, India.*

***Corresponding author**: [3] abdulhakeem6@gmail.com

Article History: Received **25** November **2017**; Accepted **06** March **2018**

Contents

1. Introduction

The Casson fluid model is one of the most commonly used rheological model and has certain advantages over non- Newtonian fluid models. This was first introduced by Casson in 1995. Casson fluid exhibits yield stress. When yield stress is dominant in contrast to shear stress this model exhibits solid like behaviour and deformation occurs when yield stress is less significant as compared to shear stress. Some examples of Casson fluid are as follows, honey, tomato sauce, soup, jelly, concentrated fruit juices, etc. Human blood can also be treated as Casson fluid. In recent years, several researchers have investigated the Casson fluid flow problem with various physical effects [1-5]. The magnetohydrodynamics flow and heat transfer for a viscous fluid has enormous applications in many engineering problems such as MHD power generators, petroleum industries, plasma studies, geothermal energy extractions, the boundary layer control in the field of aerodynamics and many others. The application of MHD principle is an important method for affecting the flow field in the desired direction by altering the structure of the boundary layer[6-16].

Hence, main objective of the present article is to study non-uniform heat source/sink effects of Casson fluid in the presence of inclined magnetic field over a stretching sheet in the existence of thermal radiation and velocity slip boundary condition is investigated. Both analytical and numerical solutions are obtained for the transformed ODE's of momentum and energy PDE's using confluent hypergeometric function

and fourth order Runge- Kutta method with shooting technique respectively.

2. Mathematical formulation

Consider a steady, laminar, two-dimensional boundary layer flow of an incompressible, Casson fluid over a stretching sheet. Aligned magnetic field of strength B_0 applied along y direction, with acute angle anγ. At $\gamma = 90^o$ this magnetic field acts like transverse magnetic field (because $sin(90^o) = 1$). The rheological equation of state for an isotropic and incompressible flow of a Casson fluid is

$\tau_{ij} = \begin{cases} 2(\mu_B + p_y/\sqrt{2\pi})e_{ij}, \pi > \pi_c \\ 2(\mu_B + p_y/\sqrt{2\pi_c})e_{ij}, \pi < \pi_c \end{cases}$ Here, $\pi = e_{ij}e_{ij}$ and e_{ij} are the (i, j) th component of the deformation rate, π is the product of the component of deformation rate with itself, π_c is a critical value of this product based on the non-Newtonian model, μ_B is plastic dynamic viscosity of the non-Newtonian fluid, and p_y is the yield stress of the fluid.

2.1 Flow Analysis

The equation governing the problem under consideration is given by

$$u_x + v_y = 0 \tag{2.1}$$

$$uu_x + vu_y = \vartheta\left(1+\beta^{-1}\right)u_{yy} - \frac{\sigma B_0^2}{\rho}\ u\ sin^2\gamma \tag{2.2}$$

where u and v are the velocity components of x and y direction, respectively, ϑ is the kinematic viscosity, ρ is the fluid density, $\beta = \mu_B\sqrt{2\pi_c}/p_y$ is the parameter of the Casson fluid and σ is the electrical conductivity. The boundary conditions for the velocity field are of the form

$$u = ax + l\frac{\partial u}{\partial y},\ \ v = v_w \ \text{ at } \ y = 0,$$
$$u \to 0 \quad \text{as} \quad y \to \infty \tag{2.3}$$

We introduce the subsequent conventional similarity transformation and dimensionless variables η and $f(\eta)$

$$u = axf_\eta, \quad v = -(a\vartheta)^{\frac{1}{2}}f, \quad \eta = \left(\frac{a}{\vartheta}\right)^{\frac{1}{2}}y \tag{2.4}$$

Using (4), (1) is trivially satisfied and (2) and (3) take the form:

$$\left(1+\frac{1}{\beta}\right)f_{\eta\eta\eta} + ff_{\eta\eta} - f_\eta^2 + Mnsin^2\gamma f_\eta = 0 \tag{2.5}$$

with corresponding boundary conditions

$$f = 0,\ \ f_\eta = 1 + Lf_{\eta\eta}, \quad \text{at} \quad \eta = 0,$$
$$f_\eta \to 0 \quad \text{as} \quad \eta \to \infty \tag{2.6}$$

The subscript η denotes differentiation with respect to η. Here $Mn = \dfrac{\sigma B_0^2}{\rho a}$ is the magnetic parameter. $L = l\sqrt{\dfrac{a}{\vartheta}}$ is the slip parameter.

The solution of (5) subject to boundary conditions is (6) can be found in the form,

$$f(\eta) = X\left(\frac{1-e^{-\alpha\eta}}{\alpha}\right) \tag{2.7}$$

Where

$$X = \frac{1}{L\alpha+1}$$
$$\alpha = -\frac{1}{3L} - \frac{2^{1/3}\alpha_1}{3L(1+\beta)\left(\alpha_2+\sqrt{\left(\alpha_2^2+4\alpha_1^3\right)^{1/3}}\right)}$$
$$+\frac{\alpha_2+\sqrt{\left(\alpha_2^2+4\alpha_1^3\right)^{1/3}}}{3(2)^{1/3}(L+L\beta)}$$
$$\alpha_1 = -(1+\beta)^2 - 3LMn\beta(L+L\beta)sin^2\gamma$$
$$\alpha_2 = -2-6\beta+27L^2\beta-6\beta^2+54L^2\beta^2$$
$$-2\beta^3+27L^2\beta^3+18L^2Mn\beta sin^2\gamma$$
$$+36L^2M\beta^2sin^2\gamma+18L^2Mn\beta^3sin^2\gamma$$

The wall shearing stress on the surface of the stretching sheet is given by

$$\tau_w = \left[v\left(\frac{\partial u}{\partial y}\right)\right]_{y=0} \tag{2.8}$$

The local skin friction coefficient is given by

$$C_f = \frac{\tau_w}{\rho {u_w}^2} = {Re_x}^{-1/2}\left(1+\frac{1}{\beta}\right)f_{\eta\eta}(0) \tag{2.9}$$

where $Re_x = \dfrac{xu_w}{\vartheta}$ is the Reynolds number.

2.2 Heat Transfer Analysis

The governing thermal boundary layer equation of incompressible Casson fluid are stated as follows:

$$\rho c_p(uT_x + vT_y) = kT_{yy} - q_{ry} + q''' \tag{2.10}$$

where k is the thermal conductivity, ρ is the density, T is the temperature and c_p is the specific heat of constant pressure.

q''' is the space and temperature dependent internal heat generation/absorption (non-uniform heat source/sink) which can be expressed in simplest form as

$$q''' = \left(\frac{ku_w(x)}{x\nu}\right)[A^*(T_w - T_\infty)f_\eta + B^*(T - T_\infty)] \tag{2.11}$$

where A^* and B^* are parameters of the space and temperature dependent internal heat generation/absorption. It is to be noted that $A^* > 0$ and $B^* > 0$ correspond to internal heat generation while $A^* < 0$ and $B^* < 0$ correspond to internal absorption.

The Rosseland diffusion approximation for radiation heat flux has given by

$$q_r = -\frac{4\sigma^*}{3k^*}\frac{\partial T^4}{\partial y}, \tag{2.12}$$

where σ^* is the Stefan-Boltzmann constant and k^* is the mean absorption coefficient. Further, we assume that the temperature difference within in flow is such that T^4 may be expanded

in a Taylor series. Hence expanding T^4 about T_∞ and neglecting higher order terms we get

$$T^4 \cong 4{T_\infty}^3 T - 3T_\infty^4. \tag{2.13}$$

The boundary conditions are given by

$$\begin{array}{l} T = T_w = T_\infty + A(\frac{x}{l})^2 \quad \text{at} \quad y = 0, \\ T \to T_\infty \text{ as } \quad y \to \infty \end{array} \tag{2.14}$$

where T_w is the temperature of the sheet, T_∞ is the temperature of the fluid far away from the sheet and l is the characteristic length. Define the non-dimensional temperature $\theta(\eta)$ as

$$(T_w - T_\infty)\,\theta(\eta) = T - T_\infty. \tag{2.15}$$

Now, we make use of the transformations given by (4), (11), (12), (15) in (10). This leads to the non dimensional form of temperature equation as follows:

$$\omega\theta_{\eta\eta} + Prf\theta_\eta - 2Prf_\eta\theta + A^* f_\eta + B^*\theta = 0, \tag{2.16}$$

where $Pr = \dfrac{\mu c_p}{k}$ is the Prandtl number, $N = \dfrac{k^* k}{4\sigma^* {T_\infty}^3}$ is radiation parameter and $\omega = \left(\dfrac{3N+4}{3N}\right)$.

Consequently the boundary conditions in (14) take the form,

$$\begin{array}{l} \theta(\eta) = 1 \ \text{ at } \ \eta = 0, \\ \theta(\eta) \to 0 \ \text{ as } \ \eta \to \infty. \end{array} \tag{2.17}$$

The solution of (16), subject to boundary conditions in (17) can be obtained in terms of confluent hypergeometric function as

$$\begin{array}{l} \theta(\eta) = c_1 e^{-\alpha\left(\frac{a_0+b_0}{2}\right)\eta} \\ \qquad \times M\left(\frac{a_0+b_0-4}{2}, 1+b_0, \frac{-Pr}{\omega\alpha^2}Xe^{-\alpha\eta}\right) \\ c_2 e^{-\alpha\eta} - c_3 e^{-2\alpha\eta} \end{array} \tag{2.18}$$

where $a_0 = Pr\left(\dfrac{X}{\omega\alpha^2}\right)$,

$$b_0 = \sqrt{a_0^2 - \frac{4B^*}{\omega\alpha^2}},$$

$$c_3 = \frac{A^* X}{\omega\alpha^2\left(1 - a_0 + \frac{B^*}{\omega\alpha^2}\right)}$$

$$c_2 = \frac{A^* X^2 Pr}{\omega^2\alpha^4\left(1 - a_0 + \frac{B^*}{\omega\alpha^2}\right)\left(4 - 2a_0 + \frac{B^*}{\omega\alpha^2}\right)}$$

$$c_1 = \frac{1 + c_2 + c_3}{M\left(\frac{a_0+b_0-4}{2}, 1+b_0, \frac{-Pr}{\omega\alpha^2}X\right)}$$

The non-dimensional wall temperature gradient obtained as follows:

$$\begin{array}{rcl} \theta_\eta(0) & = & -c_1\alpha\left(\dfrac{a_0+b_0}{2}\right) \\ & & \times M\left(\dfrac{a_0+b_0-4}{2}, 1+b_0, \dfrac{-Pr}{\omega\alpha^2}X\right) \\ & & +c_1\dfrac{PrX}{\omega\alpha}\left(\dfrac{a_0+b_0-4}{2(1+b_0)}\right) \\ & & M\left(\dfrac{a_0+b_0-2}{2}, 2+b_0, \dfrac{-Pr}{\omega\alpha^2}X\right) \\ & & +c_2\alpha + 2c_3\alpha \end{array}$$

The local heat flux can be expressed as

$$\begin{array}{l} q_w = -\left(k + \dfrac{16\sigma^* T_\infty^3}{3kk^*}\right)\left(\dfrac{\partial T}{\partial y}\right)_{y=0} \\ = -k\sqrt{\dfrac{a}{\nu}}\,(T_w - T_\infty)\left(\dfrac{3N+4}{3N}\right)\theta_\eta(0). \end{array} \tag{2.19}$$

The local Nusselt number is defined as

$$Nu_x = \frac{q_w x}{k(T_w - T_\infty)}.$$

In the present case it is derived as

$$Nu_x Re_x^{-1/2} = -\theta_\eta(0)\left(\frac{3N+4}{3N}\right).$$

3. Numerical Analysis

Employing the R.K method with shooting technique to the non dimensional ODEs along with boundary conditions, the numerical solution are obtained for different set of parameters. We have compared the values of $-\theta_\eta(0)$ with these of Turkyilmazoglu [12] for Newtonian fluid ($\beta \to \infty$) in the absence of aligned angle, velocity slip, non-uniform heat source/ sink and radiation parameters. The comparison is found to be in good agreement as shown in Table 1.

4. Results and Discussion

Fig. 1 shows the effect of magnetic parameter and angle parameter on velocity profile. It is noted that the rising of magnetic parameter reduces the velocity profile. This is due to the fact the increase in magnetic parameter, Lorentz force increases and it produces more resistance to the flow. The presence of inclined magnetic field leads to decrease the momentum boundary layer thickness. Effects of Casson parameter and slip parameter on velocity profile are plotted in Fig. 2. It is clear from the figure both parameters decrease the momentum boundary layer. Because, when slip occurs, the flow velocity near the sheet is no longer equal to the stretching velocity of the sheet. With the slip velocity increases and consequently fluid velocity decreases because under the slip condition, the pulling of the stretching sheet can be only partly transmitted to the fluid.

The effect of magnetic and angle parameters on the temperature profile is presented in Fig. 3. Due to enhancement of magnetic field strength, a resistive type force called Lorentz force associated with the aligned magnetic field makes the boundary layer thinner. Magnetic field lines of force move past the stretching sheet at the free stream velocity. The temperature profile increases with the increase of magnetic field. The combined effect of magnetic and aligned angle parameter increases the thermal boundary layer thickness. Fig. 4 demonstrates the effect of Casson and slip parameters on temperature profiles. The combined effects of Casson and slip parameters lead to increase the thickness of thermal boundary layer.

The effect of non-uniform heat source/sink with slip parameters is illustrated in Fig. 5. The temperature rises in the case of $A^* > 0$ and $B^* > 0$ heat source and gets reduce in the case of $A^* < 0$ and $B^* < 0$, heat sink. The combined effect of slip parameter with non-uniform heat source/sink parameters always lead to thickening of the thermal boundary layer.

Fig. 6 depicts the effect of Prandtl number and radiation parameter on temperature profile. The temperature profile decreases with the increasing values of radiation parameter and same trend is observed on the Prandtl number. This is due to the fact that thermal boundary layer thickness decreases as radiation and Prandtl number as increases.

Fig. 7 shows the combined effects of magnetic field with aligned angle, Casson parameter and the slip parameter on the local skin friction coefficient. The magnetic parameter Mn is taken as x-axis and the local skin friction coefficient is taken as y-axis. It is clear that the local skin friction decreases with the increasing values of Mn and γ. The local skin friction coefficient enhances with the slip and Casson parameter and reduces with magnetic parameter.

Effect of non-uniform heat source/sink parameters A^* and B^* on the local Nusselt number are shown in Fig. 8. The magnetic parameter Mn is taken as x-axis and the local Nusselt number is taken as y-axis. The combined effect of magnetic parameter and non-uniform heat source/sink parameter are reducing the local Nusselt number.

5. Conclusion

Aligned magnetic field effects on Casson fluid flow over a stretching sheet with non-uniform heat source/sink. Both analytical and numerical solutions are obtained for governing momentum and energy equations and the following specific results are obtained.

- The velocity of the non-Newtonian fluid reduces with the increasing aligned angle of magnetic field, Casson parameter, slip parameter and magnetic parameter.
- The inclined angle of the magnetic field plays a vital role in controlling the magnetic field strength and the effects of Lorentz force on the Casson fluid flow region.
- The temperature profile enhances with the increasing values of aligned angle of magnetic field, Casson param-

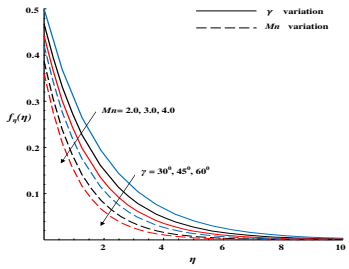

Fig: 1 Effect of magnetic and angle parameters on velocity profile $f(\eta)$ with $L = 2$, $\beta = 0.5$, Mn=1 and $\gamma = 45^0$.

Figure 1. Effect of Slip and Casson parameters on velocity profile $f_\eta(\eta)$ with $L = 2, \beta = 0.5, Mn = 1$ and $\gamma = 45^0$.

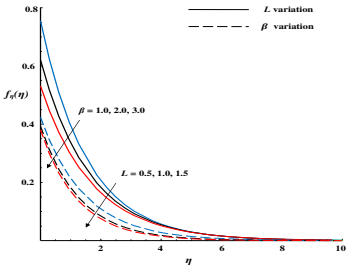

Fig: 2 Effect of Slip and Casson parameters on velocity profile $f_\eta(\eta)$ with $L = 2$, $\beta = 0.5$, Mn=1 and $\gamma = 45^0$.

Figure 2. Effect of magnetic and angle parameters on velocity profile $f_\eta(\eta)$ with $L = 2, \beta = 0.5, Mn = 1$ and $\gamma = 45^0$.

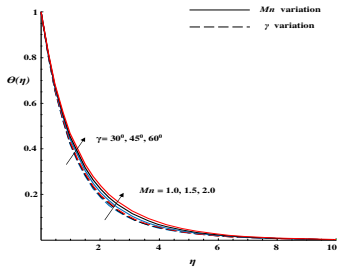

Fig. 3 Effect of magnetic and angle parameters on temperature profile $\Theta(\eta)$ with $L = 0.2$, $\beta = 0.3$, N=5, A*=0.1, B*=0.1, Pr= 0.71, Mn=0.4 and $\gamma = 45^0$.

Figure 3. Effect of Slip and Casson parameters on temperature profile $\theta(\eta)$ with $L = 0.2, \beta = 0.3, N = 5, A^* = 0.1, B^* = 0.1, Pr = 0.71, Mn = 0.4$ and $\gamma = 45^0$.

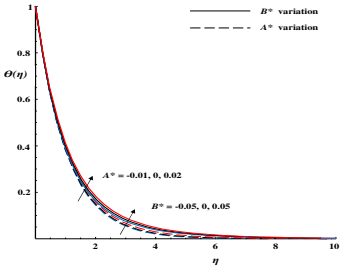

Fig: 5 Effect of A* and B* parameters on temperature profile $\Theta(\eta)$ with $L = 0.2$, $\beta = 0.3$, N=5, A*=0.1, B*=0.1, Pr= 0.71, Mn=0.4 and $\gamma = 45^0$.

Figure 5. Effect of A^* and B^* parameters on temperature profile $\theta(\eta)$ with $L = 0.2, \beta = 0.3, N = 5, A^* = 0.1, B^* = 0.1, Pr = 0.71, Mn = 0.4$ and $\gamma = 45^0$.

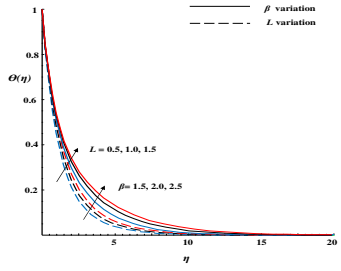

Fig: 4 Effect of Slip and Casson parameters on temperature profile $\Theta(\eta)$ with $L = 0.2$, $\beta = 0.3$, N=5, A*=0.1, B*=0.1, Pr= 0.71, Mn=0.4 and $\gamma = 45^0$.

Figure 4. Effect of magnetic and angle parameters on temperature profile $\theta(\eta)$ with $L = 0.2, \beta = 0.3, N = 5, A^* = 0.1, B^* = 0.1, Pr = 0.71, Mn = 0.4$ and $\gamma = 45^0$.

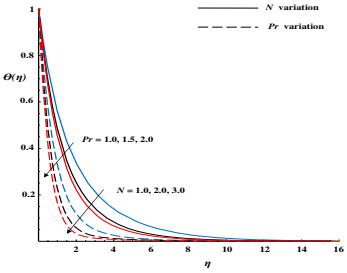

Fig: 6 Effect of Prandtl number and radiation parameters on temperature profile $\Theta(\eta)$ with $L = 0.2$, $\beta = 0.3$, N=5, A*=0.1, B*=0.1, Pr= 0.71, Mn=0.4 and $\gamma = 45^0$.

Figure 6. Effect of Prandtl number and radiation parameter on temperature profile $\theta(\eta)$ with $L = 0.2, \beta = 0.3, N = 5, A^* = 0.1, B^* = 0.1, Pr = 0.71, Mn = 0.4$ and $\gamma = 45^0$.

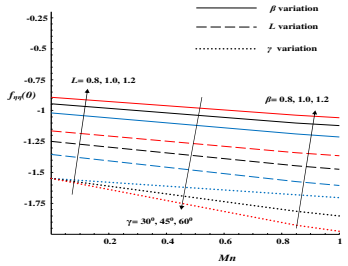

Fig: 7 Effect of magnetic, Slip, angle and Casson parameters on local skin-friction $f_{\eta\eta}(\theta)$ with β =0.3, L=0.5 and $\gamma = 45^0$.

Figure 7. Effect of magnetic, Slip, angle and Casson parameters on local skin-friction $f_{\eta\eta}(0)$ with $\beta = 0.3, L = 0.5$ and $\gamma = 45^0$

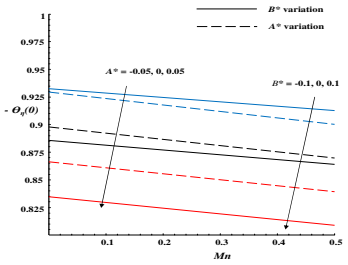

Fig: 8 Effect of magnetic, A* and B* parameters on local Nusselt number with $L = 0.5, \beta = 0.3, N$=4, A*=0.1, B*=0.1, Pr= 0.71 and $\gamma = 45^0$.

Figure 8. Effect of magnetic, A^* and B^* parameters on the local nusslt number with $L = 0.5, \beta = 0.3, N = 4, A^* = 0.1, B^* = 0.1, Pr = 0.71$ and $\gamma = 45^0$.

eter, velocity slip parameter, magnetic and non- uniform heat source/sink parameters and decreases with Prandtl number and radiation parameter.

- An enhancement in the aligned angle of magnetic field decreases the local skin friction.
- The non-uniform heat source/sink parameter decreases the local Nusselt number.

Table 1. Comparison of $-\theta_\eta(0)$

Mn	Pr	Turkyilmazoglu [8]	Analytical	Numerical
0	1	1.33333	1.33333	1.33333
	5	3.31648	3.31648	3.31648
1	1	1.21577	1.21577	1.21577
	5	———	3.20720	3.20720

Acknowledgment

One of the authors (A.K.A.H.) gratefully acknowledges the financial support of minor research project, UGC, New Delhi, India under UGC/SERO/MRP-6729/16 for pursuing this work.

References

[1] S.M. Ibrahim, G. Lorenzini, P. Vijaya Kumar, C.S.K. Raju, Influence of chemical reaction and heat source on dissipative MHD mixed convection flow of a Casson nanofluid over a nonlinear permeable stretching sheet,*Int. J. Heat Mass Transfer*, 111 (2017) 346-355.

[2] A.K. Abdul Hakeem, P. Renuka, N. Vishnu Ganesh, R. Kalaivanan, B. Ganga, Influence of inclined Lorentz forces on boundary layer flow of Casson fluid over an impermeable stretching sheet with heat transfer,*J. Magn. Magn. Mater.,* 401 (2016) 354-361.

[3] A. Zaib, M.M. Rashidi, A.J. Chamkha, K. Bhattacharyya, Numerical solution of second law analysis for MHD Casson nanofluid past a wedge with activation energy and binary chemical reaction, *Int. J. Numer. Method Heat Fluid Flow* , 27(12) (2017) , 2816-2834.

[4] R. Kalaivanan, P. Renuka, N. Vishnu Ganesh, A.K. Abdul Hakeem, B. Ganga, S. Saranya, Effects of Aligned Magnetic Field on Slip Flow of Casson Fluid over a Stretching Sheet, *Procedia Eng.,* 127 (2015) 531-538.

[5] A. J. Benazir, R. Sivaraj, M.M. Rashidi, Comparison between Casson fluid flow in the presence of heat and mass transfer from a vertical cone and flat plate,*J. Heat Transfer Transactions ASME*, 138(11) (2016), 1–6.

[6] M. Sheikholeslami, D.D. Ganji, M. Younus Javed, R. Ellahi, Effect of thermal radiation on magnetohydrodynamics nanofluid flow and heat transfer by means of two phase model, *J. Magn. Magn. Mater.*, 374 (2015), 36-43.

[7] B. Ganga, S. Mohamed Yusuff Ansari, N. Vishnu Ganesh, A.K. Abdul Hakeem, MHD flow of Boungiorno model nanofluid over a vertical plate with internal heat generation/absorption, *Propul. Power Res.,* 5 (3) (2016) 211-222.

[8] M.M. Rashidi, S. Bagheri, E. Momoniat, N. Freidoonimehr, Entropy analysis of convective MHD flow of third grade non-Newtonian fluid over a stretching sheet,*Ain Shams Eng. J.*, 8 (1) (2017), 77-85.

[9] M.M. Rahman, Heat transfer in $Fe_3O_4 - H_2O$ nanofluid contained in a triangular cavity under a sloping magnetic field, *SQU J. for Sci.*, 23(1) (2018), 56-67.

[10] A.K. Hakeem, R. Kalaivanan, B. Ganga, N. Vishnu Ganesh, Elastic Deformation Effects on Heat and Mass Fluxes of Second Grade Nanofluid Slip Flow Controlled by Aligned Lorentz Force, *J. of Nanofluids*, 7 (2) (2018), 325-337.

[11] B.J. Gireesha, B. Mahanthesh, I.S. Shivakumara, K.M. Eshwarappa, Melting heat transfer in boundary layer stagnation-point flow of nanofluid toward a stretching sheet with induced magnetic field, *Eng. Sci. Tech. Int. J.,* 19 (1) (2016) 313-321.

[12] M. Turkyilmazoglu, Analytic heat and mass transfer of the mixed hydro-dynamic/ thermal slip MHD viscous flow over a stretching sheet, *Int. J. Mech. Sci.,* 53 (2011), 886-896.

[13] A.K. Hakeem, R. Kalaivanan, N. Vishnu Ganesh, B. Ganga, Effect of partial slip on hydromagnetic flow over a porous stretching sheet with non-uniform heat source/sink, thermal radiation and wall mass transfer, *Ain Shams Eng. J.*, 5 (3)(2014), 913-922.

[14] M. Sheikholeslami, Hari R. Kataria, Akhil S. Mittal, Effect of thermal diffusion and heat-generation on MHD nanofluid flow past an oscillating vertical plate through porous medium, *J. Molecular Liq.,* 257 (2018), 12-25.

[15] M.J. Uddin, M.M. Rahman, M.S. Alam, Analysis of natural convective heat transport in a homocentric annuli containing nanofluids with an oriented magnetic field using nonhomogeneous dynamic model, *Neural Computing and Applications*, (2017), 1-20. DOI 10.1007/s00521-017-2905-z.

[16] M. Sheikholeslami, M.M. Rashidi, D.D. Ganji, Effect of non-uniform magnetic field on forced convection heat transfer of Fe3O4-water nanofluid, *Comput. Method Appl. M.*, 294 (2015) 299-312.

★★★★★★★★★
ISSN(P):2319 – 3786
Malaya Journal of Matematik
ISSN(O):2321 – 5666
★★★★★★★★★